Polymer Chemistry

Accepted Manuscript

This article can be cited before page numbers have been issued, to do this please use: G. Yu, Y. Tian, K. Li and D. Chen, *Polym. Chem.*, 2024, DOI: 10.1039/D4PY01369G.

ROYAL SOCIETY OF CHEMISTRY

rsc.li/polymers

Organocatalyzed Photoredox Radical Cyclopolymerization of Methacrylate- and Acrylamide-Crotonate Hybrid Monomers

Gaoyuan Yu,[a†] Yong-Le Tian,[b†] Ke Li,[c] Dian-Feng Chen*[c]

[a]Department of Thyroid and Breast Surgery, Affiliated Anhui Provincial Hospital, Anhui Medical University, Hefei 230032, China.

[b]College of Chemistry and Chemical Engineering, Qingdao University, Qingdao 266071, China.

[c]Hefei National Research Center of Physical Sciences at the Microscale and Department of Polymer Science and Engineering, University of Science and Technology of China, Hefei, Anhui 230026, China. E-mail: cdf@ustc.edu.cn.

[†]These authors contributed equally to this work.

ABSTRACT

Cascade bond-forming polymerizations have emerged as a powerful strategy for the synthesis of polymeric materials with advanced structures and properties. Among these, radical cyclopolymerization is one of the most extensively studied methodologies, though it still faces several challenges, including low cyclization rates, unwanted crosslinking, and lack of spatiotemporal control. Herein, we report the design and synthesis of methacrylate- and acrylamide-crotonate hybrid monomers, which undergoes in a visible light-driven, organocatalyzed photoredox ATRP-type cyclopolymerization. This approach eliminates crosslinking and proceeds through a sophisticated sequence of intramolecular cyclization and intermolecular propagation, yielding diverse homopolymers and block copolymers with cyclic repeating units. Additionally, factors influencing the control over polymer chain growth, such as light

View Article Online
DOI: 10.1039/D4PY01369G

intensity and additives, are explored.

INTRODUCTION

The merger of reversible-deactivation radical polymerization (RDRP) with visible-light photocatalysis has been recognized as a mild and versatile strategy for synthesizing polymers with diverse structures and functionalities.[1 –7] This approach not only imparts excellent control over polymer chain growth, tailoring the molecular weights (MWs) and narrowing the molecular weight distributions,[8] but also provides unique spatiotemporal control which enables a broad scope of applications ranging from photolithography to 3D manufacturing.[9–12] Among the numerous mechanisms employed in photocontrolled RDRP, atom transfer radical polymerization (ATRP) is one of the most extensively studied controlled radical polymerization methodologies.[6,13] In contrast to the early ATRP examples mediated by Cu(I)[14] or Ru(II)[15] complexes under thermal conditions, the development of photocontrolled ATRP has focused on two dimensions: sustainable photoredox processes and an expanded monomer scope. To address concerns about transition metal contaminations, considerable efforts have been directed toward the development of efficient photocatalysts (PCs), shifting from metal complexes [16–22] to metal-free systems. As such, a variety of purely organic molecules, including perylene,[23 –24] phenothiazines,[25–2728] dihydrophenazines,[29 –30] phenoxazines,[31 –32] carbazoles,[33] thieothiophenes,[34] dihydroacridines,[35] and oxygen-/sulfur-doped polycyclic arenes,[36–37] have proven effective and practical for organocatalyzed ATRP (O-ATRP), yielding well-defined polymers with high chain-end fidelity and controlled topology. On the other hand, methacrylates have dominated the research of O-ATRP, while progress involving other vinyl monomers (e.g., acrylates,[27–28, 35, 38] acrylamides,[39–40] acrylonitrile,[26,41] and styrene[23–33]) remains limited. Expanding the scope of

View Article Online
DOI: 10.1039/D4PY01369G

polymerizable monomers, particularly those with intriguing polymerizability profiles, is highly desirable for further advancing this field.

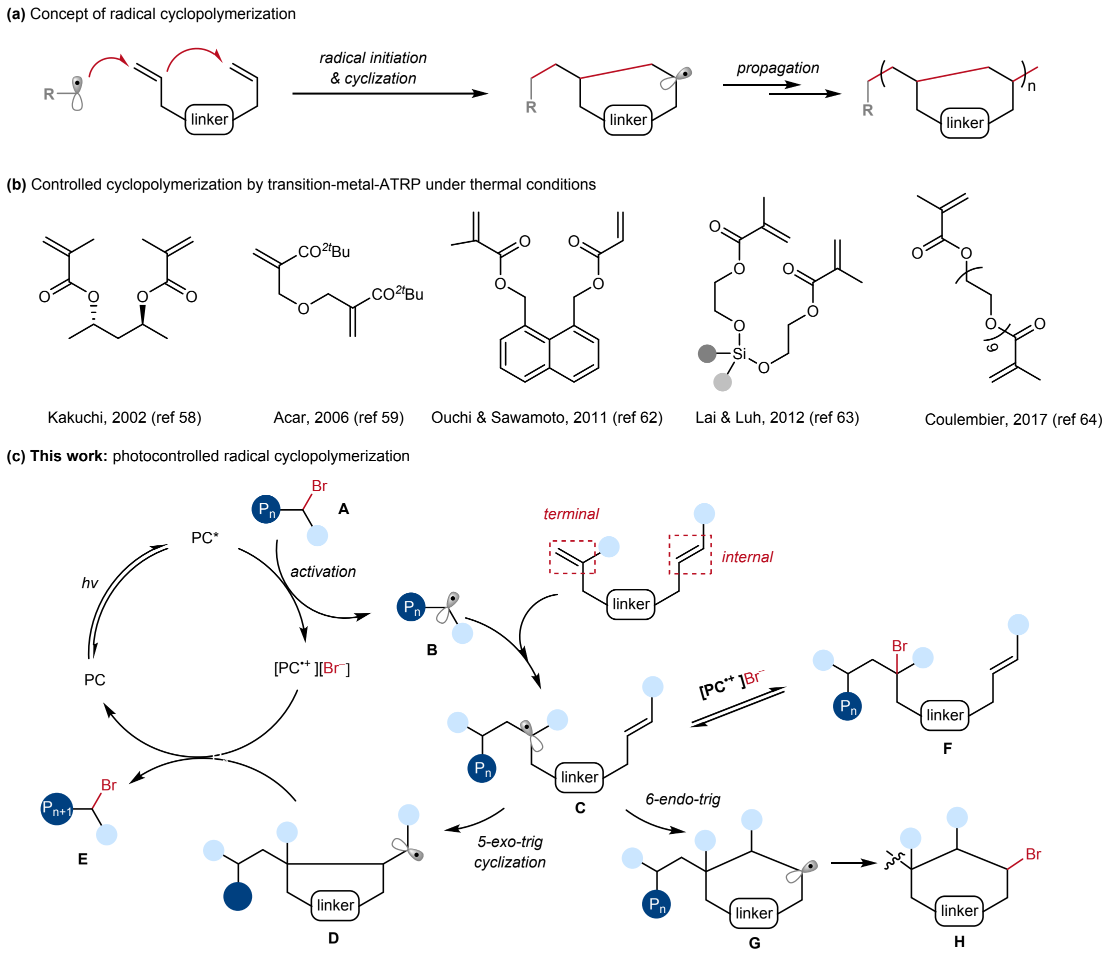

Fig. 1 **(a)** Concept of radical cyclopolymerization. **(b)** Cyclopolymerization using transition-metal-based ATRP technology. **(c)** Photocontrolled radical cyclopolymerization in this work.

In contrast to conventional single-reactivity monomers, multi-functionalized molecules hold the potential for cascade reactions in polymerizations, leading to advanced polymers with unique structures and properties.[42–45] A premier example is the radical cyclopolymerization of diene monomers, where sequential intramolecular cyclization and propagation ideally proceed to afford linear polymers with cyclic repeating units (Fig. 1a).[46] In the realm of free-radical cyclopolymerization, various divinyl monomers have been designed to (a) enable the direct preparation of functional polymeric materials, such as poly(diallyldimethylammoniumchloride)[47] and its

View Article Online
DOI: 10.1039/D4PY01369G

copolymers with acrylamide for water treatment, and (b) address the alternation challenge in copolymerization of two distinct vinyl monomers through an alternating intra-intermolecular chain mechanism. Additionally, conventional nitroxide-mediated radical polymerization (NMP),[48] reversible addition-fragmentation chain transfer (RAFT),[49–57] and ATRP[58–64] techniques have been applied to radical cyclopolymerization, offering precise control over MWs, dispersities, and chain-end livingness, which enables sequence-defined copolymerization (Fig. 1b). Despite these advancements, a photocontrolled radical cyclopolymerization has yet been realized, likely due to long-standing problems, such as low cyclization rates and inevitable crosslinking, which complicate the process and hinder the effective control by a photocatalyst.

We hypothesized that a vinyl monomer bearing a pendent internal alkene functionality would help minimize these unwanted side reactions in radical cyclopolymerizaiton. As depicted in Fig. 1c, a highly reducing PC in its excited state (PC*) can donate an electron to the dormant chain-end bromide **A**, thus generating a propagating carbon radical **B** and the $[PC^{\bullet+}][Br^{-}]$ complex. Upon vinyl addition of species **B** to the monomer, intermediate **C** is formed, which afterwards can undergo multiple pathways: (a) radical species may be recaptured by the $[PC^{\bullet+}][Br^{-}]$ complex, (**C** to **F**); (b) **C** may cyclize in a 5-*exo-trig* manner (**C** to **D**) or (c) a 6-endo-trig manner (**C** to **G**). Notably, the direct radical addition of **B** to the pendent internal C–C double, which exhibits higher steric hindrance than the adjacent vinyl group, should be kinetically unfavorable. Finally, deactivation of radical species **D** and **G** by $[PC^{\bullet+}][Br^{-}]$ results in the formation of dormant polymer **E** and **H**, respectively. Given the limited redox window of commonly used PCs, the resulting inactive alkyl chain-end bromide **H** is unlikely to be re-activated for propagation,[65] representing an unwanted pseudo-

View Article Online
DOI: 10.1039/D4PY01369G

termination pathway. In this work, we report the synthesis of malonate-linked methacrylate-crotonate and *p*-toluenesulfonamide-linked acrylamide-crotonate monomers, and their highly selective radical cyclopolymerization by using a visible-light-drien photoredox ATRP approach.

RESULTS AND DISCUSSION

Initial radical cyclopolymerization of M1

To valid our hypothesis, **M1**, diethyl-2-bromo-2-methylmalonate (DBMM), and *N,N′*-di(2-naphthyl)dihydrophenazine (**1**)[29] were selected as the monomer, initiator and photocatalyst, respectively. Gratifyingly, a 0.5 mmol-scale polymerization of **M1** under conditions of [**M1**]/[DBMM]/[**1**] = 500/10/1 in 1.0 mL of *N,N*-dimethylacetamide (DMAc), with white LEDs irradiation (~10.8 W) and a fan to maintain the temperature ~ 30 °C, proceeded smoothly and reached 81% monomer conversion to give highly soluable **PM1** with a number-average molecular weight (M_n) of 8.7 kDa and a moderate dispersity ($Đ$) of 1.60 (Table 1, entry 1). The ^{1}H NMR spectrum of obtained **PM1** (Fig. S44) showed no signal of vinyl or alkenyl protons, suggesting an exclusive cyclopolymerizaton rather than the vinyl polymerization. As mentioned in Fig. 1c, cyclopentyl and cyclohexyl units are likely formed *via* 5-*exo-trig*- and 6-*endo-trig* cyclization, respectively. However, due to their high structural similarity, the ratios of these two units cannot be determined based on the ^{1}H NMR spectrum of **PM1**. Inspired by Niu's[56] and Huang's[66] strategy that utilizes a small-molecule model reaction to illustrate the structure of complex polymers, we performed a photoredox-catalyzed stoichiometric reaction of **M1** with a glycine derivative[67] as the radical precursor (Fig. 2). This reaction afforded 5-membered product **2a** as a ~ 4:1 mixture of diastereomers in 44% yield, while its six-membered analogous product **2b** was not observed (Fig. S10–11), indicating a favorable 5-*exo-trig* reaction pathway. Accordingly, the core

View Article Online
DOI: 10.1039/D4PY01369G

structure of repeating units of obtained **PM1** was assigned as cyclopentane.

Table 1 Photocontrolled radical cyclopolymerization of **M1**[a]

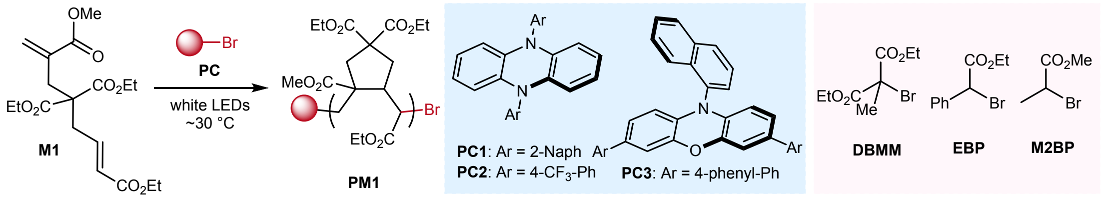

entry	PC	initiator	[**M1**]/[**I**]/[**PC**]	solvent	Conv. (%)[b]	$M_{n,theo}$ (kDa)[c]	M_n (kDa)[d]	Đ[d]
1	**PC1**	DBMM	500/10/1	DMAc	81	15.2	8.7	1.60
2	**PC1**	DBMM	500/10/1	EtOAc	91	16.9	14.6	1.85
3	**PC1**	DBMM	500/10/1	PhCl	92	17.3	15.1	1.59
4	**PC2**	DBMM	500/10/1	PhCl	85	16.0	15.7	1.70
5	**PC3**	DBMM	500/10/1	PhCl	89	16.7	12.7	1.64
6	**PC1**	EBP	500/10/1	PhCl	76	14.3	12.4	1.60
7	**PC1**	M2BP	500/10/1	PhCl	64	12.0	11.3	1.66
8[e]	**PC1**	DBMM	500/10/1	PhCl	0	-	-	-
9	**-**	DBMM	500/10/1	PhCl	0	-	-	-
10	**PC1**	-	500/10/1	PhCl	0	-	-	-
11	**PC1**	DBMM	500/25/1	PhCl	96	7.4	7.2	1.59
12	**PC1**	DBMM	1000/10/1	PhCl	71	26.5	15.4	1.68
13	**PC1**	DBMM	2000/10/1	PhCl	38	28.3	13.2	1.63

[a] Polymerizations performed using 0.5 mmol of **M1**, 0.0025–0.025 mmol of alkyl bromide, 0.001 mmol of PC, 1.0 mL of solvent, and irradiated by white LEDs (~10.8 W) for 12 h. A cooling fan was used to maintain the temperature ~30 °C. No [b] Measured by crude ^{1}H-NMR. [c] $M_{n,theo}$ = MW(initiator) + MW(**M1**) × conversion × ([**M1**]/[initiator]). [d] Determined by gel permeation chromatography (GPC) in THF (1.0 mL/min, 40 °C) and calibrated with polystyrene standards. [e] In the dark.

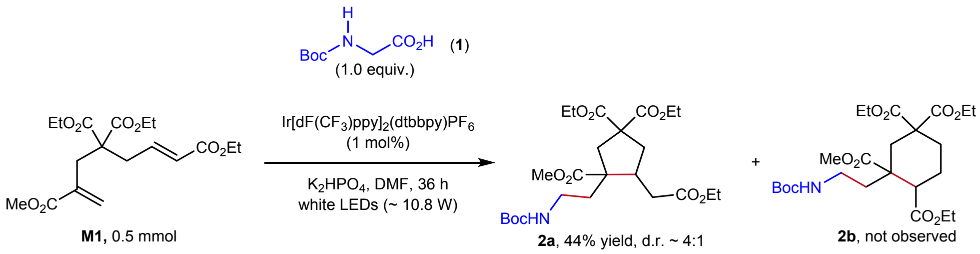

Fig. 2 Model reaction of **M1** with glycine derivative **2** under photoredox conditions

Effect of solvents, photocatalysts, and initiators

A brief screening of solvents (Table, entries 1–3) suggested that chlorobenzene

View Article Online
DOI: 10.1039/D4PY01369G

(PhCl) was superior to others in achieving higher monomer conversion (92%) and producing **PM1** with a M_n (15.1 kDa) close to its theoretical value and a lower *Đ* of 1.59 (entry 3). Replacing **PC1** with *N,N′*-di(4-CF_3-phenyl)dihydrophenazine (**PC2**) or core-modified *N*-(1-naphthyl)phenoxazine (**PC3**) led to slightly decreased monomer conversions and higher-dispersity (*Đ* = 1.64–1.70, entries 4–5). Examination of other commonly used O-ATRP alkyl bromide initiators, including ethyl α-bromophenylacetate (EBP) and methyl 2-bromopropionate (M2BP), revealed that DBMM outperformed these initiators, affording polymers with the best monomer conversion and dispersity (entries 6–7 vs entry 3). Importantly, the radical cyclopolymerization did not proceed in the absence of light (entry 8), PC (entry 8), or initiator (entry 10), providing strong evidence for the photoredox ATRP mechanism. Additionally, polymerization performed with [**M1**]/[DBMM]/[**1**] = 500/25/1 produced **PM1** with predictable M_n = 7.2 kDa and moderate *Đ* = 1.59 (entry 11), while attempts to target higher degree of polymerization (DP) were unsuccessful (entries 12–13), probably due to increased termination events.

Investigation on the role of light intensity

Compared to typical O-ATRP, which produces well-defined poly(methacrylates) with *Đ* < 1.2, this photoredox radical cyclopolymerization of **M1** generally afforded **PM1** with *Đ* ~ 1.6. This higher dispersity is likely due to the incorporation of the crotonate moiety, which introduces a secondary radical species that is structurally similar to the propagating radical in ATRP of acrylates. Since the propagating rate constant (k_p) of acrylates is an order of magnitude higher than that for methacrylates,[68] the chain growth through crotonate-to-methacrylate cross propagation is challenging to control. In addition, the occasional formation of six-membered cyclic repeating units (**C** to **G** to **H**, Fig. 1c) likely contributes to chain termination, further complicating the control of polymer chain growth.

To gain deeper insights into the overall control of the polymerization, several experiments were performed. First, the role of light intensity in the polymerization of [**M1**]/[DBMM]/[**1**] = 500/10/1 in PhCl at ~30 °C was investigated. In fact, first-order

View Article Online
DOI: 10.1039/D4PY01369G

kinetics were revealed for polymerizations conducted under white LEDs irradiation ranging from 1.4 to 10.8 W (Fig. 3a). The rates of polymerization roughly correlated to the intensity of irradiation and decreased with lower light intensity, as it actually influences the concentration of excited-state PC,[69] which in turn regulate the radical cyclopolymerization. Importantly, two **PM1** samples, synthesized under 10.8 W (Fig. 3b) and 1.4 W irradiation (Fig. 3c), were analyzed by matrix-assisted laser desorption ionization time of flight mass (MALDI-TOF MS) spectrometry. The analyses revealed that increased light intensity can accelerate side reactions, such as radical coupling and hydrogen atom abstraction to form a C–H chain end.

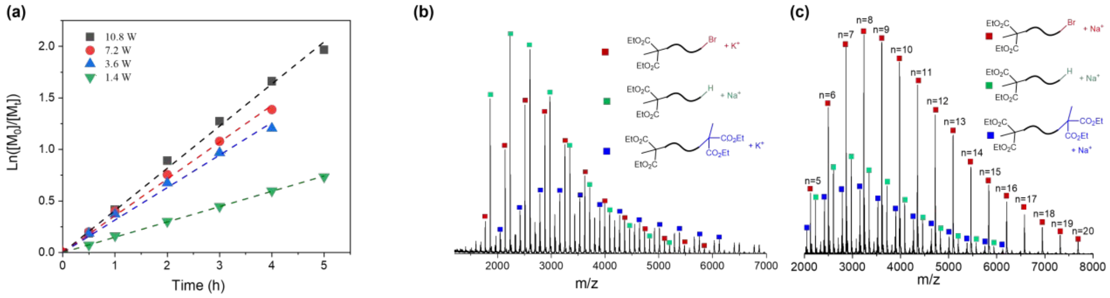

Fig. 3 (a) Plots of natural log of monomer conversion as a function of time for polymerizations of [**M1**]/[DBMM]/[**PC1**] = 500/10/1 performed in PhCl (0.5 M), at ~30 °C, with 1.4–10.8 W white LED irradiation. MALDI-TOF MS spectra of low-MW **PM1** synthesized with **(b)** 10.5 W and **(c)** 1.4 W white LEDs irradiation.

Kinetic study and chain-end fidelity

We then monitored the polymerization of [**M1**]/[DBMM]/[**PC1**] = 500/10/1 in PhCl (0.5 M), at ~30 °C, with 1.4 W white LED irradiation. First, a linear increase in polymer MW as a function of monomer conversion was observed (Fig. 4a), demonstrating the robustness of O-ATRP process. Second, a pulsed irradiation experiment was performed, where the cyclopolymerization proceeded with light, paused in the dark, and revived upon re-irradiation (Fig. 4b and 4c). Third, the excellent chain-end fidelity allowed chain extension with methyl methacrylate (MMA) using an isolated **PM1** (M_n = 4.9 kDa, $Đ$ = 1.60) as the macroinitiator (Fig. 4d). The gel-

View Article Online
DOI: 10.1039/D4PY01369G

permeation chromatography (GPC) traces before and after the chain extension confirmed the successful preparation of a block copolymer **PM1**-*b*-**PMMA** (Fig. 4e).

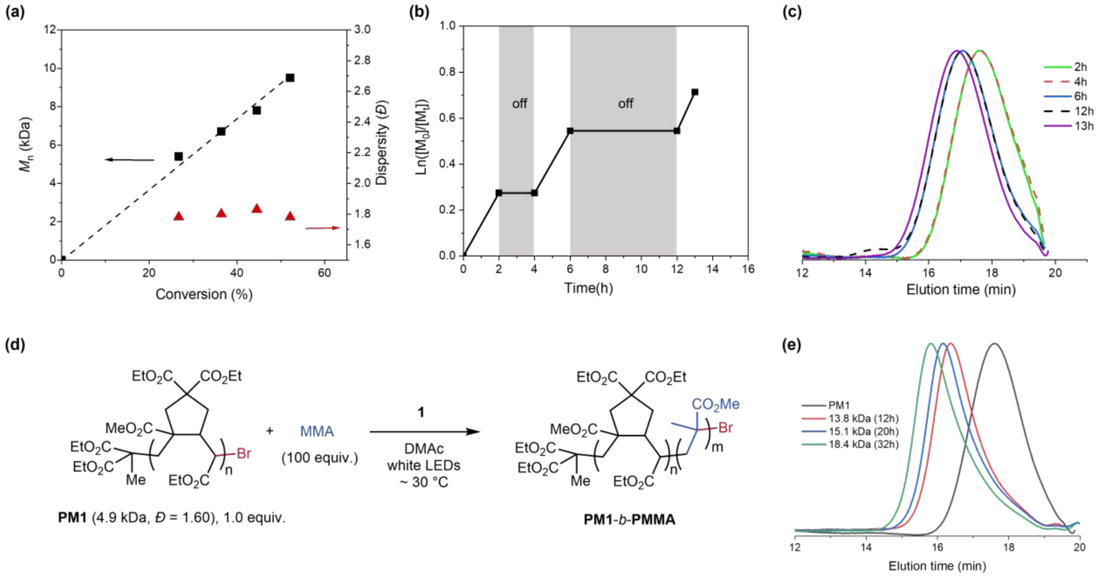

Fig. 4 **(a)** Plots of measured M_n and $Đ$ as a function of monomer conversion for polymerization of [**M1**]/[DBMM]/[**PC1**] = 500/10/1 performed in PhCl (0.5 M), at ~30 °C, with 1.4 W white LED irradiation. **(b)** Plots of natural log of monomer conversion as a function of time and **(c)** overlayed GPC traces for pulsed irradiation experiment. **(d)** Chain-extension polymerization from a **PM1** macroinitiator with MMA. **(e)** Overlayed GPC traces for chain-extension polymerization.

Effect of bromide additives

From the perspective of reversible-deactivation mechanism in ATRP, the addition of bromide salts primarily shifts the equilibrium to the dormant Br chain ends, thereby enhancing control over the polymer chain growth.[35] We investigated the effects of LiBr on cyclopolymerization of [**M1**]/[DBMM]/[**1**] = 500/10/1 in PhCl at ~30 °C under ~ 1.4 W white LED irradiation (Table 2, entries 1–3). The inclusion of LiBr, regardless of its concentration, unexpectedly led to an increase in dispersity, probably due to its poor solubility in PhCl. In polymerizations of **M1** performed in EtOAc, the polymerization rates negatively correlated to the concentration of LiBr, although the dispersities of obtained **PM1** remained high (entries 4–6). We then turned to

View Article Online
DOI: 10.1039/D4PY01369G

tetrabutylammonium bromide (TBAB) as an additive. Encouragingly, despite a reduction in monomer conversion, the addition of 3.0 equiv. of TBAB to DBMM resulted in the formation of **PM1** with a M_n of 11.8 kDa and a low $Đ$ of 1.38 (entry 9). More importantly, the MALDI-TOF MS analysis of low molecular-weight **PM1** synthesized under such conditions (entry 9) indicated high chain-end fidelity (Fig. S3), underscoring the importance of the bromide anion in the photoredox deactivation process.

Table 2 Effect of bromide additives on photoredox radical cyclopolymerization of **M1**[a]

entry	additive	solvent	[**M1**]/[DBMM]/[**1**][**Br**]	Conv.%[b]	$M_{n,theo}$ (kDa)[c]	M_n (kDa)[d]	$Đ$[d]
1	LiBr	PhCl	500/10/1/10	79	14.9	13.4	1.91
2	LiBr	PhCl	500/10/1/20	77	14.5	11.9	1.90
3	LiBr	PhCl	500/10/1/30	76	14.3	12.1	1.97
4	LiBr	EtOAc	500/10/1/10	77	14.5	11.8	1.79
5	LiBr	EtOAc	500/10/1/20	65	12.3	7.5	1.95
6	LiBr	EtOAc	500/10/1/30	55	10.4	7.4	1.96
7	TBAB	PhCl	500/10/1/10	79	14.9	15.1	1.59
8	TBAB	PhCl	500/10/1/20	85	16.0	13.6	1.48
9	TBAB	PhCl	500/10/1/30	68	12.8	11.8	1.38

[a]Polymerizations performed using 0.5 mmol of **M1**, 0.01 mmol of DBMM, 0.001 mmol of **1**, 0.01–0.03 mmol of bromide additive, 1.0 mL of PhCl, and irradiated by white LEDs (~1.4 W) for 12 h. A cooling fan was used to maintain the temperature ~30 °C. [b]Measured by crude ^{1}H-NMR. [c]$M_{n,theo}$ = MW(initiator) + MW(**M1**) × conversion × ([**M1**]/[initiator]). [d]Determined by gel permeation chromatography (GPC) in THF (1.0 mL/min, 40 °C) and calibrated with polystyrene standards. [e]In EtOAc.

Scope of methacrylate-crotonate diene monomers

With optimized conditions in hand, we next explored the generality of this radical cyclopolymerization method. Diene monomers containing methyl- (**M2**), benzyl- (**M3**), and *tert*-butyl crotonate (**M4**) motifs were successfully polymerized by using this organocatalyzed photoredox protocol, affording corresponding **PM2**–**PM4** of 10.3–

View Article Online
DOI: 10.1039/D4PY01369G

17.2 kDa and with moderate dispersitis ~ 1.5. It is noteworthy that the monomer structure significantly impacts the polymerizability. First, the substituent effect of the crotonate motif was observed. Compared to **M2** and **M3**, **M4** bearing a sterically bulky *tert*-butyl group exhibited lower reactivity under identical polymerization conditions, as evidenced by lower monomer conversion (80%). Second, the linker's chemical structure principally dominates the monomer's cyclopolymerizability. For instance, polymerization of **M5**, which contains a cyanoacetate linkage, proceeded more slowly, reaching only 45% conversion to produce **PM5** with M_n = 4.5 kDa and $Đ$ = 1.58. In contrast, polymerizations of *p*-toluenesulfonamide-linked **M6** and acrylamide-crotonate monomer **M7** achieved near quantitative conversions, yielding **PM6** (M_n = 7.1 kDa and $Đ$ = 1.66) and **PM7** (M_n = 22.2 kDa and $Đ$ = 1.80), respectively. Finally, a block copolymer **PM1-*b*-PM6** (M_n = 12.0 kDa and $Đ$ = 1.57) was successfully synthesized using **PM1** (M_n = 5.3 kDa and $Đ$ = 1.71) as the macroinitiator and **M6** as the comonomer, as evidenced by the shift of retention time in the GPC traces before and after the copolymerization (Fig. S9).

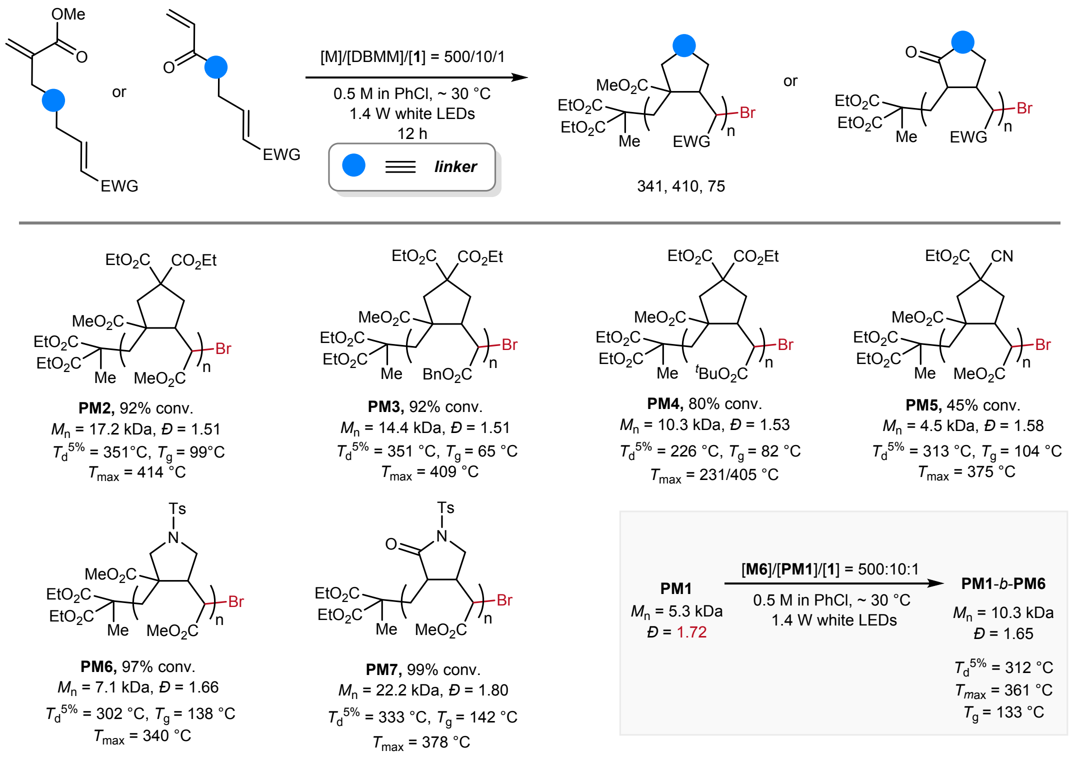

View Article Online
DOI: 10.1039/D4PY01369G

Fig. 5 Monomer Scope

The thermal properties of obtained polymers were then investigated. First, the thermal stability of **PM1**–**PM7** was examined by thermogravimetric analysis (TGA) in terms of decomposition temperature at 5% weight loss ($T_d^{5\%}$) and maximum decomposition temperature (T_{max}), which is defined as the peak value in relative derivative thermogravimetry (DTG). **PM1**–**PM3** generally exhibited high $T_d^{5\%}$ of 314–351 °C and T_{max} of 409–410 °C, while those of **PM4** significantly decreased to 226 °C and 231 °C, respectively, probably due to the fast decomposition of the pendant *tert*-butyl group. Nitrogen-containing polymers, **PM5**–**PM7**, seem to be less stable in terms of lower $T_d^{5\%}$ (302–333 °C) and T_{max} (340–378 °C). Second, the glass transition temperatures (T_gs) of **PM1**–**PM4** were measured by differential scanning calorimetry (DSC), ranging from 65 to 99 °C. The T_gs of nitrogen-containing **PM5**–**PM7** (104 to 142 °C) are higher than those bearing cyclopentane units, indicating the presence of more rigid cyclic structures.

EXPERIMENTAL

Material and methods

All Chemicals were purchased from TCI, J&K, Energy Chemical, and Adamas-beta, and were used as received without further purification. All synthesis and handle of air- and moisture-sensitive chemicals were performed in a N_2-filled glove box.

^{1}H NMR and ^{13}C NMR spectroscopy

^{1}H NMR and ^{13}C NMR spectra were recorded on a Bruker 400 Hz (100 Hz for ^{13}C) spectrometer at ambient temperature. Chemical shifts (δ) for both ^{1}H and ^{13}C NMR spectra were given in ppm relative to tetramethylsilane. All NMR spectra were referenced to the residual solvent ($CHCl_3$) signal (δ = 7.26 ppm for ^{1}H NMR and δ = 77.00 ppm for ^{13}H NMR).

View Article Online
DOI: 10.1039/D4PY01369G

Gel permeation chromatography (GPC)

Analysis of polymer's number-average molecular weight (M_n) and dispersity ($Đ$) was performed using a Waters e2695 system (with one guard column and two Styragel columns) coupled with Waters 2414 refractive index detector (calibrated with 10 polystyrene standards). The analysis was performed at 40 °C using THF as the eluent at a flow rate of 1.0 mL/minute.

Thermo-gravimetric analysis (TGA)

Decomposition temperatures ($T_d^{5\%}$) at 5% of weight loss and maximum rate decomposition temperatures (T_{max}) of the obtained polymers were measured by thermal gravimetric analysis (TGA) on a TA Q50 analyzer, TA instruments. Polymer samples were measured by heating the polymer samples from 25 °C to 700 °C at the rate of 10 °C/min.

Differential scanning calorimetry (DSC)

Glass transition temperatures (T_g) of obtained polymers were measured by differential scanning calorimetry (DSC) on a TA Q20 analyzer, at a rate of 10 °C/min. All T_g values were obtained from a second scan.

CONCLUSIONS

In summary, we have designed and synthesized a series of diene monomers that integrate methacrylates or acrylamide with crotonates. By using *N,N′*-di(2-naphthyl)dihydrophenazine **1** as the photocatalyst and DBMM as the initiator, radical polymerization of these hybrid monomers proceed exclusively through a sequence of intramolecular cyclization and intermolecular propagation, resulting in polymers with unique cyclic repeating units. Kinetic studies, along with the effects of light intensity and bromide additives, combined with MALDI-TOF mass spectrometry analysis, have provided valuable insights into this radical cyclopolymerization driven by the

View Article Online
DOI: 10.1039/D4PY01369G

photoredox ATRP mechanism. This approach enables straightforward synthesis of a range of novel homopolymers and block copolymers with low to moderate dispersities. With these findings presented in this work, we believe that photocontrolled radical cyclopolymerization is a promising and practical strategy for accessing new polymeric materials with distinct properties.

Author Contributions

G.-Y. and Y.-L. T. performed the experiments. G.-Y., Y.-L. T. and K. L. analyzed the data. D.-F. C. directed the project, and wrote the manuscript with assistance from all authors. G.-Y. and Y.-L. T. contributed equally to this work.

Conflicts of interest

The authors declare no competing financial interest.

Data availability

The data supporting this article have been included as part of the Supplementary Information.

Acknowledgements

This work was financially supported by the NSFC (grant no. 22101273) and the Fundamental Research Fund for the Central Universities (WK9990000111). This work was partially carried out at the Instruments Center for Physical Science, University of Science and Technology of China (USTC).

REFERENCES

---

1 F. A. Leibfarth, K. M. Mattson, B. P. Fors, H. A. Collins and C. J. Hawker, *Angew. Chem. Int. Ed.,* 2013, **52,** 199–210.

2 X. Pan, M. A. Tasdelen, J. Laun, T. Junkers, Y. Yagc and K. Matyjaszewski, K. *Prog. Polym.*

Sci., 2016, **62,** 73–125.

3 M. Chen, M. Zhong and J. A. Johnson, *Chem. Rev.,* 2016, **116,** 10167−10211.

4 S. Dadashi-Silab, S. Droan and Y. Yagci, *Chem. Rev*., 2016, **116,** 10212–10275.

5 N. Corrigan, S. Shanmugam, J. Xu and C. Boyer, *Chem. Soc. Rev.,* 2016, **45,** 6165−6212.

6 D. A. Corbin and G. M. Miyake, *Chem. Rev.,* 2022, **122,** 1830–1874.

7 Q. Michaudel, V. Kottisch and B. P. Fors, *Angew. Chem., Int. Ed.*, 2017, **56**, 9670–9679.

8 Y. Zhou, J. L , Y. Wu and Z. Luo, *Chem. Rev*., 2020, **5**, 2950–3048.

9 J. E. Poelma, B. P. Fors, G. F. Meyers, J. W. Kramer and C. J. Hawker, *Angew. Chem., Int. Ed.*, 2013, **52**, 6844–6848.

10 C. W. Pester, B. Narupai, K. M. Mattson, D. P. Bothman, D. Klinger, K. W. Lee, E. H. Discekici and C. J. Hawker, *Adv. Mater.*, 2016, **28**, 9292–9300.

11 E. H. Discekici, C. W. Pester, N. J. Treat, J. Lawrence, K. M. Mattson, B. Narupai, E. P. Toumayan, Y. Luo, A. J. McGrath, P. G. Clark, J. Read de Alaniz and C. J. Hawker, *ACS Macro Lett.*, 2016, **5**, 258–262.

12 J. Yan, X. Pan, M. Schmitt, Z. Wang, M. R. Bockstaller and K. Matyjaszewski, *ACS Macro Lett.*, 2016, **5**, 661–665.

13 E. H. Discekici, A. Anastasaki, J. Read De Alaniz and C. J. Hawker, *Macromolecules,* 2018, **51,** 7421–7434.

14 J.-S. Wang and K. Matyjaszewski, *J. Am. Chem. Soc.,* 1995, **117,** 5614–5615.

15 M. Kato, M. Kamigaito, M. Sawamoto and T. Higashimura, Macromolecules, 1995, **28**, 1721–1723.

16 D. Konkolewicz, K. Schroder, J. Buback, S. Bernhard and K. Matyjaszewski, *ACS Macro Lett.,* 2012, **1**, 1219−1223.

17 J. Mosnáček and M. Ilčíková, *Macromolecules,* 2012, **45,** 5859−5865.

18 A. Anastasaki, V. Nikolaou, Q. Zhang, J. Burns, S. R. Samanta, C. Waldron, A. J. Haddleton, R. McHale, D. Fox, V. Percec, P. Wilson and D. M. Haddleton, *J. Am. Chem. Soc.,* 2014, **136,** 1141−1149.

19 B. P. Fors and C. J. Hawker, *Angew. Chem. Int. Ed.* 2012, **51,** 8850−8853.

20 X. Pan, N. Malhotra, J. Zhang and K. Matyjaszewski, *Macromolecules*, 2015, **48**, 6948–6954.

21 S. Dadashi-Silab, X. Pan and K. Matyjaszewski, *Macromolecules,* 2017, **50,** 7967–7977.

22 K. Parkatzidis, S. Boner, H. S. Wang and A. Anastasaki, *ACS Macro Lett.,* 2022, **11,** 841–846.

23 G. M. Miyake and J. C. Theriot, *Macromolecules,* 2014, **47,** 8255–8261.

24 C. Aydogan, G. Yilmaz and Y. Yagci, *Macromolecules*, 2017, **50**, 9115 —9120.

25 N. J. Treat, H. Sprafke, J. W. Kramer, P. G. Clark, B. E. Barton, J. Read de Alaniz, B. P. Fors and C. J. Hawker, *J. Am. Chem. Soc.,* 2014, **136**, 16096–16101.

26 X. Pan, M. Lamson, J. Yan and K. Matyjaszewski, *ACS Macro Lett.,* 2015, **4,** 192–196.

27 Y. C. Zhao, H. H. Gong, K. M. Jiang, S. J. Yan, J. Lin and M. Chen, *Macromolecules*, 2018, **51**,

View Article Online
DOI: 10.1039/D4PY01369G

938–946.

28 H. Zhou, L. Zhang, P. Wen, Y. Zhou, Y. Zhao, Q. Zhao, Y. Gu, R. Bai and M. Chen, *Angew. Chem. Int. Ed.,* 2023, **62**, e202304461.

29 J. Theriot, C.-H. Lim, H. Yang, M. Ryan, C. Musgrave and G. Miyake, *Science,* 2016, **352**, 1082–1086.

30 C.-H. Lim, M. D. Ryan, B. G. McCarthy, J. C. Theriot, S. M. Sartor, N. H. Damrauer, C. B. Musgrave and G. M. Miyake, *J. Am. Chem. Soc.,* 2017, **139**, 348–355.

31 R. M. Pearson, C.-H. Lim, B. G. McCarthy, C. B. Musgrave and G. M. Miyake, *J. Am. Chem. Soc.,* 2016, **138**, 11399–11407.

32 B. G. McCarthy, R. M. Pearson, C. H. Lim, S. M. Sartor, N. H. Damrauer and G. M. Miyake, *J. Am. Chem. Soc.*, 2018, **140**, 5088–5101.

33 V. K. Singh, C. Yu, S. Badgujar, Y. Kim, Y. Kwon, D. Kim, J. Lee, T. Akhter, G. Thangavel and L. S. Park, *Nat. Catal.*, 2018, **1**, 794–804.

34C. Kutahya, A. Allushi, R. Isci, J. Kreutzer, T. Ozturk, G. Yilmaz and Y. Yagci, *Macromolecules*, 2017, **50**, 6903–6910.

35 B. L. Buss, C. H. Lim and G. M. Miyake, *Angew. Chem., Int. Ed.*, 2020, **59**, 3209–3217.

36 Q. Ma, J. Song, X. Zhang, Y. Jiang, L. Ji and S. Liao, *Nat. Commun.,* 2021, **12**, 429.

37 H. Shao, S. Li, Y. Jiang, J. Song, X. Zhang, J. Chen and S. Liao. *Polym. Chem.,* 2024, **15**, 4134–4140.

38 B. McCarthy, S. Sartor, J. Cole, N. Damrauer and G. M. Miyake. *Macromolecules,* 2020, **53**, 9208−9219.

39 C. Aydogan, C. Kutahya, A. Allushi, G. Yilmaz and Y. Yagci, *Polym. Chem.*, 2017, **8**, 2899–2903.

40 Y. Xu, G. Li, Y. Hu and Y. Wang, *Macromol. Chem. Phys.*, 2018, **219**, 1800192.

41 D. Wei, Y. Xu, C. Liu, Y. Zhai, H. Chen, L. Bai, H. Yang, L. Yang, W. Wang and Y. Niu. *J. Polym. Sci., Part A: Polym. Chem.,* 2019, **57**, 1265–1269.

42 J. S. Yuan, W. Q. Wang, Z. F. Zhou and J. Niu, *Macromolecules*, 2020, **53**, 5655–5673.

43 G. I. Peterson and T. L. Choi, *Chem. Sci.*, 2020, **11**, 4843–4854.

44 G. Chen, L. Xia, F. Wang, Z. Zhang and Y.-Z. You, *Polym. Chem.*, 2021, **12**, 3740–3752.

45 D.-Y. Zhang and D.-F. Chen, *J. Funct. Polym.,* 2023, **36**, 261–274.

46 D. Pasini and D. Takeuchi, *Chem. Rev.*, 2018, **118**, 8983–9057.

47 G. B. Butler and R. J. Angelo, *J. Am. Chem. Soc.*, 1957, **79**, 3128−3131.

48 Y. Kametani, M. Nakano, T. Yamamoto, M. Ouchi and M. Sawamoto, *ACS Macro Lett.,* 2017, **6**, 754−757.

49 P. Gerdt and A. Studer, *Angew. Chem. Int. Ed.,* 2022, **61**, e202206964.

50 Y. Assem, H. Chaffey-Millar, C. Barner-Kowollik, G. Wegner and S. Agarwal, *Macromolecules*, 2007, **40**, 3907–3913.

View Article Online
DOI: 10.1039/D4PY01369G

51 Y. Assem, A. Greiner and S. Agarwal, *Macromol. Rapid Commun.*, 2007, **28**, 1923–1928.

52 S. Erkoc and A. E. Ouchi, *Macromolecules,* 2008, **41**, 9019–9024.

53 J. Li, M. Du, Z. Zhao and H. Liu, *Macromolecules,* 2016, **49**, 445−454.

54 Y. Kametani, M. Sawamoto and M. Ouchi, *Angew. Chem. Int. Ed.,* 2018, **57**, 10905–10909.

55 Y. Kametani, Kametani, F. Tournilhac, M. Sawamoto and M. Ouchi, *Angew. Chem. Int. Ed.,* 2020, **59**, 5193–5201.

56 H. Huang, W. Wang, Z. Zhou, B. Sun, M. An, F. Haeffner and J. Niu, *J. Am. Chem. Soc.*, 2019, **141**, 12493–12497.

57 Y. Wang, J. Du and H. Huang. *Angew. Chem. Int. Ed.,* 2024, **63**, e202318898.

58 M. Tsuji, R. Sakai, T. Satoh, H. Kaga and T. Kakuchi, *Macromolecules,* 2002, **35**, 8255–8257.

59 S. Erkoc, L. J. Mathias and A. E. Acar, *Macromolecules,* 2006, **39**, 8936–8942.

60 Y. Hibi, M. Ouchi and M. Sawamoto, *Angew. Chem., Int. Ed.,* 2011, **50**, 7434–7437.

61 M. Ouchi, M. Nakano, T. Nakanishi and M. Sawamoto, *Angew. Chem., Int. Ed.,* 2016, **55**, 14584−14589.

62 Y. Hibi, S. Tokuoka, T. Terashima, M. Ouchi and M. Sawamoto, *Polym. Chem.,* 2011, **2**, 341–347.

63 Z. Hu, Y.-P. Xu, D. Wu, B. Li, Y.-C. Huang, J.-X. Jiang, G.-Q. Lai and T.-Y. Luh, *Macromol. Chem. Phys.,* 2012, **213**, 566−571.

64 S. Moins, J. C. Martins, A. Krumpmann, V. Lemaur, J. Cornil, N. Delbosc, A. Decroly, Ph. Dubois, R. Lazzaroni, J.-F. Gohy and O. Coulembier, *Chem. Commun.,* 2017, **53**, 6899–6902.

65 D.-F. Chen, B. M. Boyle, B. G. McCarthy, C.-H. Lim and G. M. Miyake, *J. Am. Chem. Soc.*, 2019, **141**, 13268–13277.

66 S. Zhang, C. Cao, S. Jiang and H. Huang, *Macromolecules,* 2022, **55**, 9411−9419.

67 L. Chu, C. Ohta, Z. Zuo, D. W. C. MacMillan, *J. Am. Chem. Soc.*, 2014, **136**, 10886–10889.

68 W. Tang and K. Matyjaszewski, *Macromolecules,* 2007, **40**, 1858–1863.

69 M. D. Ryan, R. M. Pearson, T. A. French and G. M. Miyake, *Macromolecules,* 2017, **50**, 4616−4622.

View Article Online
DOI: 10.1039/D4PY01369G

Data availability

The data supporting this article have been included as part of the Supplementary Information.